Robust Model Predictive Control Framework for Energy-Optimal Adaptive Cruise Control of Battery Electric Vehicles

Sheng Yu, Xiao Pan, Anastasis Georgiou, Boli Chen, Imad M. Jaimoukha and Simos A. Evangelou

***Abstract*— The autonomous vehicle following problem has been extensively studied for at least two decades with the rapid development of intelligent transport systems. In this context, this paper proposes a robust model predictive control (RMPC) method that aims to find the energy-efficient following velocity of an ego battery electric vehicle and to guarantee a safe rear-end distance in the presence of disturbances and modelling errors. The optimisation problem is formulated in the space domain so that the overall problem can be convexified in the form of a semi-definite program, which ensures a rapid solving speed and a unique solution. Simulations are carried out to provide numerical comparisons with a nominal model predictive control (MPC) scheme. It is shown that the RMPC guarantees robust constraint satisfaction for the closed-loop system whereas constraints may be violated when the nominal MPC is in use. Moreover, the impact of the prediction horizon length on optimality is investigated, showing that a finely tuned horizon could produce significant energy savings.**

I. INTRODUCTION

Thanks to the recent development of Vehicle-to-Vehicle (V2V) communication technologies [1], real-time vehicle information including velocity, position and trajectory can be transmitted among vehicles [2]. It is therefore of great interest to study how improvements in road vehicle control can be made with the information accessed by V2V and Vehicle-to-Infrastructure (V2I) connectivity. Of particular interest is adaptive cruise control (ACC), which involves determining an optimal driving speed during car-following paradigms with consideration of various aspects, such as energy-efficiency, safety and comfort [3], [4], [5].

When eco-driving and ACC are fused (namely eco-ACC), it leads to a constrained control/optimisation problem for which model predictive control (MPC) has been known as one of the most preferable solution methods. Over the past decade, numerous MPC-based approaches have been proposed for this problem [4], [6], [7], [8], [9], [10]. In particular, reference [4] proposed a multi-objective MPC algorithm that optimises a weighted sum of fuel-economy, comfort and safety properties for conventional vehicles. The trade-off between tracking capability and the fuel economy is investigated in [9] while other important aspects such as ride comfort and driver acceptable tracking error are taken into account by input and state constraints. Moreover, the work presented in [10] compared driving performances of an MPC method and human drivers and showed that the MPC controller can operate more safely than real drivers without sacrificing passenger comfort.

Despite the rich literature in MPC-based ACC strategies, ubiquitous modelling uncertainties and external disturbances are not taken into consideration until recent years [11], [12], [13], [14], [15]. More specifically, in [13], the authors proposed a tube-based robust MPC method to solve vehicle following problems subject to inaccurate or delayed information of the lead vehicle and modelling errors. An alternative tube-based MPC was proposed in [14], where two types of disturbances are addressed including both unmodelled dynamics and traffic perturbations, such as cut-in, lane change and emergency braking. A disturbance predictor has been integrated in the MPC proposed in [15] so as to enhance system robustness with the disturbance forecast.

Considering the nonlinearity of the vehicle longitudinal and powertrain dynamics involved in the eco-ACC problem, most of the existing MPC-based control strategies are still computationally demanding for onboard processing units of modern vehicles, particularly the nonlinear MPC approaches [16], [17], [18]. In this context, this paper deals with a computationally efficient robust MPC (RMPC) algorithm for eco-ACC. The contribution of the paper is threefold: 1) a convex eco-ACC modelling framework for an electric vehicle with consideration of various disturbances and uncertainties is developed; 2) an RMPC algorithm is designed for the ACC problem with semi-definite programming relaxation (SDPR) to formulate the control problem into linear matrix inequalities (LMIs); and 3) numerical comparisons between the robust and a nominal MPC are carried out to verify the effectiveness of the RMPC method.

The rest paper begins with a description of the vehicle following model and a convex problem formulation in Section II, and it is followed by Section III, which introduces the SDPR RMPC algorithm. Simulation results are illustrated and discussed in Section IV. Finally, conclusions are provided and a future work plan is suggested in Section V.

II. SYSTEM DESCRIPTION

A. Vehicle Following Model

This work considers the vehicle following scenario, where an ego vehicle (controlled vehicle) follows a lead vehicle (reference vehicle) with a safety inter-vehicular time gap. The space domain modelling approach is utilised to facilitate problem convexification [19]; the convexification process will be presented later in Section II-B. Let s denote the variable of travelled distance. The transformation from time to space domain is achieved by changing the independent variable of time t to s via $\frac{d}{ds} = \frac{1}{v}\frac{d}{dt}$. Further consider m the mass of the controlled vehicle. It is convenient to use

S. Yu, X. Pan, A. Georgiou, I. M. Jaimoukha and S. A. Evangelou are with the Dept. of Electrical and Electronic Engineering at Imperial College London, UK (sheng.yu17@ic.ac.uk, xiao.pan17@ic.ac.uk, anastasis.georgiou16@ic.ac.uk, i.jaimouka@ic.ac.uk, s.evangelou@ic.ac.uk)

B. Chen is with the Dept. of Electronic and Electrical Engineering at University College London, UK (boli.chen@ucl.ac.uk)

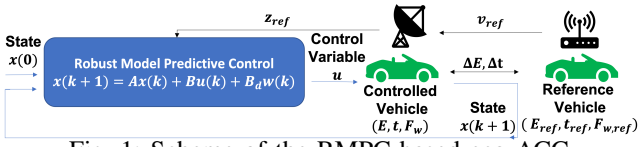

Fig. 1: Scheme of the RMPC-based eco-ACC.

as a state variable the kinetic energy $E(s)=\frac{1}{2}mv^2(s)$ in the space domain instead of the variable $v(s)$, the linear (forward) velocity of the controlled vehicle.

Fig. 1 shows the scheme of the vehicle following problem with the V2V communication system. Past information containing kinetic energy $E_{ref}(s)$ and travelled time $t_{ref}(s)$ of the reference vehicle are shared with the controlled vehicle. Note that the communication through the V2V system in this work is assumed to be ideal with no delays. For safety purposes and the feasibility of the V2V communication range, the following constraint is imposed:

$$\frac{\Delta v(s)}{|a_{w,\min}|}+T_\sigma \leq \Delta t(s) \leq \Delta t_{max} \tag{1}$$

where $\Delta t(s)=t(s)-t_{ref}(s)$ is the time gap between the two vehicles at distance s, $\Delta v(s)=v(s)-v_{ref}(s)$ is the corresponding velocity difference with $v(s)=\sqrt{2E(s)/m}$, $v_{ref}(s)=\sqrt{2E_{ref}(s)/m_{ref}}$, and m_{ref} is the mass of the reference vehicle. Moreover, $a_{w,\min}=\frac{F_{w,\min}}{m}$ is the maximum allowed deceleration, with $F_{w,\min}$ the maximum braking force (it has a negative value), such that the force acting on the wheels (driving or braking), $F_w \geq F_{w,\min}$. T_σ is the braking response time of the vehicle braking system (lag between driver braking command and braking system response) [19]. As such, the left hand side of (1) is the time-to-collision (TTC) constraint designed for the controlled vehicle to avoid a potential rear-end collision. The right hand side of (1) is a designed upper bound of $\Delta t(s)$ where its value is determined by considering the traffic flow rate [20], the driver preference [21], as well as the V2V communication range [22].

Instead of utilising the state of the controlled vehicle ($E(s)$, $t(s)$) to construct the control problem, this work considers ($\Delta E(s)$,$\Delta t(s)$) as system states for the convenience of dealing with the influence of a potential disturbance $w(s)$ in (1):

$$\frac{d}{ds}\Delta E(s)=F_w(s)-F_{tyre}-2\frac{f_d}{m}E(s)-F_{ref}(s)+w(s), \tag{2a}$$

$$\frac{d}{ds}\Delta t(s)=\frac{1}{v(s)}-\frac{1}{v_{ref}}, \tag{2b}$$

where $\Delta E(s)=E(s)-E_{ref}(s)$ is the difference of the kinetic energies of the two vehicles, $F_{tyre}=f_T mg$ is the tyre resistance force with f_T the rolling resistance coefficient, f_d is air drag resistance coefficient [23], and $F_{ref}(s)=\frac{d}{ds}E_{ref}(s)$ is the total force of the reference vehicle. Furthermore, $w(s)\leq f_w(\overline{v_w})$ is an external disturbance caused by various reasons such as V2V communication noises, modelling mismatches and prediction errors, where $f_w(\overline{v_w})=\frac{1}{2}m\overline{v_w}^2/\Delta s$ is defined in terms of the disturbance limits on the reference vehicle speed $\overline{v_w}\in\mathbb{R}_{>0}$ and the sampling interval $\Delta s\in\mathbb{R}_{>0}$. The difference of the kinetic energies $\Delta E(s)$ and driving force $F_w(s)$ of the controlled vehicle are constrained, respectively, by permissible limits:

$$\frac{1}{2}mv_{\min}^2-E_{ref}(s)\leq\Delta E(s)\leq\frac{1}{2}mv_{\max}^2-E_{ref}(s), \tag{3a}$$

$$F_{w,\min}\leq F_w(s)\leq F_{w,\max}, \tag{3b}$$

where $v_{\min}$ and $v_{\max}$ are minimum and maximum speed limits, in which $v_{\max}$ is determined based on infrastructure requirements and traffic regulations and $v_{\min}$ is set as a sufficiently small positive value to avoid the singularity issue in (2b). Moreover, $F_{w,\max}$ is the maximum force that the powertrain is capable of delivering to the wheels [19].

In this work, we consider the controlled vehicle as a battery electric vehicle (BEV), in which the energy regeneration system is considered for the energy consumption evaluation. As such, the battery energy consumption is formulated by the "wheel-to-distance" energy losses, such that the energy dissipation function of the controlled vehicle over a specific space range $[0, s_f]$ with $s_f\in\mathbb{R}_{>0}$ is described by [24]:

$$E_b=\int_0^{s_f}F_w(s)ds, \tag{4}$$

where $F_w(s)\geq 0$ indicates discharge of the battery and $F_w(s)<0$ corresponds to braking energy recovered by the powertrain.

The objective of the vehicle following problem is to find the optimal wheel force, $F_w(s)$, that minimises a multi-objective function of the controlled vehicle, achieving driving speed and energy optimisation over the range $[0, s_f]$, expressed as follows:

$$V=W_1\int_0^{s_f}(E(s)-\frac{1}{2}m\bar{v}^2(s))^2ds+W_2E_b(s_f), \tag{5}$$

where $W_1, W_2\in\mathbb{R}_{>0}$ are weighting factors. The first term in (5) is designed for the controlled vehicle to follow a constant cruise speed $\bar{v}$, whose value is determined based on various road conditions (such as highway or urban road) and the legal speed limit, and the second term aims to minimise the battery energy consumption (4).

The main characteristic parameters of the vehicle model are summarised in Table. I.

TABLE I: PARAMETERS OF VEHICLE FOLLOWING MODEL.

description	symbols	values
controlled/reference vehicle mass	m/m_{ref}	1500 kg
tyre rolling resistance coefficient	f_T	0.01
air drag coefficient	f_d	0.36
minimum/maximum velocity	$v_{\min}/v_{\max}$	1/33 m/s
braking response time	T_σ	2 s
maximum time difference	$\Delta t_{\max}$	11 s
minimum/maximum force on wheels	$F_{w,\min}/F_{w,max}$	-4500/4500 N

B. Model Convexification

Despite the complexity introduced in the time difference constraint (1) and the dynamics system of the vehicle following model in space domain (2), this work formulates the eco-ACC problem as a convex optimisation problem by suitable approximations, to take advantage of computational efficiency and guarantee of a unique optimal solution of convex optimisation. The approximation made in this work ensures that the approximated problem is consistent and feasible to the original problem.

To convexify the nonlinearity in the state dynamics of the time difference $\Delta t(s)$ (see (2b)), an auxillary optimisation variable $\zeta(s)$ is introduced to relax the derivative of the travelled time of the controlled vehicle $\frac{d}{ds}t(s)=\frac{1}{v(s)}$:

$$\frac{d}{ds}\Delta t(s) = \zeta(s) - 1/v_{ref}\,, \tag{6a}$$

$$\zeta(s) \geq 1/\sqrt{2E(s)/m}\,, \tag{6b}$$

such that (2b) is relaxed as a linear dynamic (6a) and a convex path constraint (6b). With the introduction of $\zeta(s)$, the objective function (5) can be rewritten in a convex form with a convex function $J(s)$:

$$V=\int_0^{s_f} J(s)ds=\int_0^{s_f} W_1(E(s)-\frac{m\bar{v}^2(s)}{2})^2+W_2F_w(s)+W_3\zeta(s)ds, \tag{7}$$

where the third term aims to minimise $\zeta(s)$ to ensure the tightness of (6b), which indirectly guarantees the feasibility and conservativeness of the convex solutions. Further verification of the validity of (6b) is performed in the simulations in Section IV (see Fig. 4).

In terms of the left hand side of (1), the nonlinearity existing in the representation of the velocity of the controlled vehicle, $v(s)=\sqrt{2E(s)/m}$, can be approximated by a conservative linear relationship $f_e(E(s))=aE(s)+b$ [19], as shown in Fig. 2. Hence, the constraint of Δt can be rewritten in a convex form:

$$T_\sigma + \frac{f_e(E(s))-v_{ref}(s)}{|a_{w,\min}|} \leq \Delta t(s) \leq \Delta t_{\max}\,, \tag{8}$$

where $f_e(E(s))=aE(s)+b, \forall E(s)\in[\frac{1}{2}mv^2_{\min},\frac{1}{2}mv^2_{\max}]$ with a and b as the fitting parameters.

C. Optimisation Formulation

To counter the impact of the disturbance $w(s)$, min-max optimisation strategy is utilised to formulate the control problem. Suppose a sampling distance interval $\Delta s\in\mathbb{R}_{>0}$, and without loss of generality, it is assumed that $s_f=k_f\Delta s$ with $k_f\in\mathbb{N}_{>0}$. Thus, the convex optimisation problem with the system state $x(k)=[\Delta E(k),\Delta t(k)]^\top$ and the control input $u(k)=[F_w(k),\zeta(k)]^\top$ for any $k\in\mathbb{N}_{[0,k_f]}$ is formulated to find the optimal control input $u(k)$, under the worst case scenario caused by $w(k)$ at each step k, that minimises the objective function in discretised-form:

$$V=\sum_{k=0}^{k_f} J(k)\Delta s\,, \tag{9a}$$

$$\textbf{s.t.}\quad x(k+1)=Ax(k)+Bu(k)+B_cC(k)+B_ww(k)\,, \tag{9b}$$

$$\underline{f}(k)\leq f(x(k),u(k),w(k))\leq \overline{f}(k)\,, \tag{9c}$$

$$-\zeta(k)+1/\sqrt{2E(k)/m}\leq 0\,, \tag{9d}$$

$$x(0)=\begin{bmatrix}\Delta E(0)\\ \Delta t(0)\end{bmatrix}, x(k_f)=\begin{bmatrix}\Delta E(k_f)\\ \Delta t(k_f)\end{bmatrix}, \tag{9e}$$

where (9d) is a convex inequality constraint [25], (9e) are the boundary conditions, and the convex function $J(k)$ in (9a) is the rearrangement based on the definition of (7) in a state-space form:

$$\begin{aligned}
&J(k)=(z(k)-\bar{z}(k))^\top Q^\top Q(z(k)-\bar{z}(k))+Pz(k)+z(k)^\top P^\top,\\
&z(k)=C_zx(k)+D_{zu}u(k)+D_{zw}w(k)\,,\\
&C_z=\begin{bmatrix}1&0\\0&0\\0&0\end{bmatrix},\quad D_{zu}=\begin{bmatrix}0&0\\1&0\\0&1\end{bmatrix},\quad D_{zw}=\begin{bmatrix}0\\0\\0\end{bmatrix},
\end{aligned} \tag{10}$$

where $Q=\text{diag}\{\sqrt{W_1},0,0\}\succeq 0$, $P=[0,W_2/2,W_3/2]\succeq 0$, $z(k)=[\Delta E(k),F_w(k),\zeta(k)]^\top$ and $\bar{z}(k)=[\frac{1}{2}m\bar{v}^2-E_{ref}(k),0,0]^\top$.

The discretised dynamic equation (9b) collecting the differences of kinetic energy ΔE (2a) and travelled time Δt (6a), is specified as below:

$$\begin{aligned}
&x(k+1)=Ax(k)+Bu(k)+B_cC(k)+B_ww(k)\,,\\
&A=\begin{bmatrix}1-\frac{2f_d}{m}\Delta s & 0\\ 0 & 1\end{bmatrix}, B=\begin{bmatrix}\Delta s & 0\\ 0 & \Delta s\end{bmatrix}, B_w=\begin{bmatrix}\Delta s\\ 0\end{bmatrix},\\
&B_c=\begin{bmatrix}\Delta s & 0\\ 0 & \Delta s\end{bmatrix}, C=\begin{bmatrix}-F_{tyre}-\frac{2f_d}{m}E_{ref}(k)-F_{ref}(k)\\ -\frac{1}{\sqrt{2E_{ref}(k)/m}}\end{bmatrix}.
\end{aligned} \tag{11}$$

The inequality constraints (9c) summarises linear constraints (1) and (3) within a state-space form:

$$\begin{aligned}
&f(k)=C_fx(k)+D_{fu}u(k)+D_{fw}w(k)\,,\\
&C_f=\begin{bmatrix}1&0\\0&1\\0&0\end{bmatrix},\quad D_{fu}=\begin{bmatrix}0&0\\0&0\\1&0\end{bmatrix},\quad D_{fw}=\begin{bmatrix}0\\0\\0\end{bmatrix},
\end{aligned} \tag{12}$$

where $f(k)=[\Delta E(k),\Delta t(k),F_w(k)]^\top$ with a lower bound $\underline{f}(k)=[\frac{1}{2}v^2_{\min}-E_{ref}(k),\frac{\Delta v(s)}{|a_{w,\min}|}+T_\sigma,F_{w,\min}]^\top$ and an upper bound $\overline{f}(k)=[\frac{1}{2}v_{\max}-E_{ref}(k),\Delta t_{\max},F_{w,\max}]^\top$.

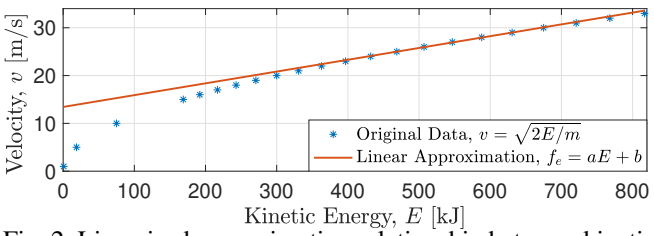

Fig. 2: Linearised approximation relationship between kinetic energy E and velocity v.

III. Robust Model Predictive Controller

In this work, we propose an RMPC scheme, as shown in Fig. 1, using SDPR [26], [27], following a similar methodology to a computationally efficient and verified scheme in non-automotive industrial applications [28]. In order to formulate the control problem into a RMPC scheme, let us first define the following stack vectors:

$$\mathbf{x}=\begin{bmatrix}x(0)\\x(1)\\\vdots\\x(N)\end{bmatrix},\mathbf{f}=\begin{bmatrix}f(0)\\f(1)\\\vdots\\f(N)\end{bmatrix},\mathbf{z}=\begin{bmatrix}z(0)\\z(1)\\\vdots\\z(N)\end{bmatrix},\mathbf{w}=\begin{bmatrix}w(0)\\w(1)\\\vdots\\w(N-1)\end{bmatrix} \tag{13}$$

and $\mathbf{C}=[C(0),\ldots,C(N-1)]^\top$, where $N\in\mathbb{N}_{>0}$ is the prediction horizon.

Using the above stacked matrix definition, the system dynamic over the prediction horizon N can be expressed as:

$$\mathbf{x}=\widetilde{A}x(0)+\widetilde{B}\mathbf{u}+\widetilde{B}_c\mathbf{C}+\widetilde{B}_d\mathbf{w}, \tag{14}$$

where $\widetilde{A}$, $\widetilde{B}$, $\widetilde{B}_c$ and $\widetilde{B}_d$ are stacked coefficient matrices and are readily obtained from iterating the dynamics in (9b). Moreover, the stacked vector $\mathbf{u}=[u(0),\ldots,u(N-1)]^\top$ represents the input signal over the prediction horizon N. Lastly, $x(0)$ represents the initial state defined in (9e). By substituting the stack vectors defined in (13) and repeating recursive steps in (12), stacked coefficient matrices $\widetilde{C}_f$, $\widetilde{D}_{fu}$ and $\widetilde{D}_{fd}$ are obtained, and hence the corresponding stacked format of the signal response function of constraints is:

$$\mathbf{f}=\widetilde{C}_f x(0)+\widetilde{D}_{fu}\mathbf{u}+\widetilde{D}_{fd}\mathbf{w}. \tag{15}$$

By using analogous methods, the stacked form of the response function of $z(k)$ in the convex function $J(k)$, which is defined in (10), can be expressed by:

$$\mathbf{z}=\widetilde{C}_z x(0)+\widetilde{D}_{zu}\mathbf{u}+\widetilde{D}_{zd}\mathbf{w}, \tag{16}$$

where $\widetilde{C}_z$, $\widetilde{D}_{zu}$ and $\widetilde{D}_{zd}$ are stacked coefficient matrices after iterating the $z(k)$ equation in (10). By substituting (10) and (16) in (9a), the cost function becomes:

$$\begin{aligned}\min_{\mathbf{u}} V=&(\widetilde{C}_z x_0+\widetilde{D}_{zu}\mathbf{u}+\widetilde{D}_{zd}\mathbf{w}-\mathbf{z}_{ref})^\top\mathbf{Q}^\top\mathbf{Q}(\widetilde{C}_z x_0+\widetilde{D}_{zu}\mathbf{u}\\&+\widetilde{D}_{zd}\mathbf{w}-\mathbf{z}_{ref})+\mathbf{P}(\widetilde{C}_z x_0+\widetilde{D}_{zu}\mathbf{u}+\widetilde{D}_{zd}\mathbf{w})\\&+(\widetilde{C}_z x_0+\widetilde{D}_{zu}\mathbf{u}+\widetilde{D}_{zd}\mathbf{w})^\top\mathbf{P}^\top,\end{aligned} \tag{17}$$

where $\mathbf{Q}$, $\mathbf{P}$ are stack matrices of the weighting matrices Q and P, respectively, and $\mathbf{z}_{ref}$ is a stacked vector of vector $\overline{z}$. Next, an auxiliary variable $\overline{\gamma}$ is defined as the upper boundary of the cost function $V\le\overline{\gamma}$ such that

$$V-\overline{\gamma}\le 0. \tag{18}$$

The semi-definite programming relaxation (SDPR) is applied to the left hand side (LHS) of the inequality in (18):

$$LHS=-(\mathbf{w}-\underline{\mathbf{w}})^\top D(\overline{\mathbf{w}}-\mathbf{w})-[\mathbf{w}^\top\ 1]L(\mathbf{u},D,\overline{\gamma})\begin{bmatrix}\mathbf{w}\\1\end{bmatrix}, \tag{19}$$

with LMI: $L(\mathbf{u},D,\overline{\gamma})=$

$$\begin{bmatrix}-\widetilde{D}_{zd}^\top\mathbf{Q}^\top\mathbf{Q}\widetilde{D}_{zd}+D & -D\frac{\mathbf{w}+\overline{\mathbf{w}}}{2}-bd\\ * & \underline{\mathbf{w}}^\top D\overline{\mathbf{w}}-cd-\mathbf{u}^\top\widetilde{D}_{zu}^\top\mathbf{Q}^\top\mathbf{Q}\widetilde{D}_{zu}\mathbf{u}+\overline{\gamma}\end{bmatrix},$$

$$\begin{aligned}bd=&\widetilde{D}_{zd}^\top\mathbf{Q}^\top\mathbf{Q}\widetilde{C}_z x_0+\widetilde{D}_{zd}^\top\mathbf{Q}^\top\mathbf{Q}\widetilde{D}_{zu}\mathbf{u}-\widetilde{D}_{zd}^\top\mathbf{Q}^\top\mathbf{Q}\mathbf{z}_{ref}+\widetilde{D}_{zd}^\top\mathbf{P}^\top,\\ cd=&x_0^\top\widetilde{C}_z^\top\mathbf{Q}^\top\mathbf{Q}\widetilde{C}_z x_0+x_0^\top\widetilde{C}_z^\top\mathbf{Q}^\top\mathbf{Q}\widetilde{D}_{zu}\mathbf{u}+\mathbf{u}^\top\widetilde{D}_{zu}^\top\mathbf{Q}^\top\mathbf{Q}\widetilde{C}_z x_0\\&-x_0^\top\widetilde{C}_z^\top\mathbf{Q}^\top\mathbf{Q}\mathbf{z}_{ref}-\mathbf{z}_{ref}^\top\mathbf{Q}^\top\mathbf{Q}\widetilde{C}_z x_0-\mathbf{u}^\top\widetilde{D}_{zu}^\top\mathbf{Q}^\top\mathbf{Q}\mathbf{z}_{ref}\\&-\mathbf{z}_{ref}^\top\mathbf{Q}^\top\mathbf{Q}\widetilde{D}_{zu}\mathbf{u}+\mathbf{z}_{ref}^\top\mathbf{Q}^\top\mathbf{Q}\mathbf{z}_{ref}\\&+\mathbf{P}(\widetilde{C}_z x_0+\widetilde{D}_{zu}\mathbf{u})+(\widetilde{C}_z x_0+\widetilde{D}_{zu}\mathbf{u})^\top\mathbf{P}^\top,\end{aligned}$$

where $*$ denotes the symmetry element of the corresponding matrix, D is a positive semi-definite diagonal matrix ($0\preceq D\in\mathbb{R}^{N\times N}$), and $\underline{\mathbf{w}}$ and $\overline{\mathbf{w}}$ are stacked vectors of the lower boundary $-|f_w(\overline{v_w})|$ and upper boundary $|f_w(\overline{v_w})|$ of the disturbance $w(s)$. In the matrix $L(\mathbf{u},D,\overline{\gamma})$, $\mathbf{u}$ is the optimal control sequence that is expected to be computed by the RMPC. However, the term $\mathbf{u}^\top\widetilde{D}_{zu}^\top\mathbf{Q}^\top\mathbf{Q}\widetilde{D}_{zu}\mathbf{u}$ is a quadratic nonlinear term, which cannot be applied in LMI optimisation. In order to eliminate the nonlinearity in $L(\mathbf{u},D,\overline{\gamma})$, Schur Complement is applied and thus, $L(\mathbf{u},D,\overline{\gamma})$ becomes:

$$L(\mathbf{u},D,\overline{\gamma})=\begin{bmatrix}-\widetilde{D}_{zd}^\top\mathbf{Q}^\top\mathbf{Q}\widetilde{D}_{zd}+D & -D\frac{\mathbf{w}+\overline{\mathbf{w}}}{2}-bd & 0\\ * & \underline{\mathbf{w}}^\top D\overline{\mathbf{w}}-cd+\overline{\gamma} & \mathbf{u}^\top\widetilde{D}_{zu}^\top\mathbf{Q}^\top\\ * & * & I\end{bmatrix}, \tag{20}$$

where $I\in\mathbb{R}^{((N+1)\times 3)\times((N+1)\times 3)}$ is an identity matrix. Since $-(\mathbf{w}-\underline{\mathbf{w}})^\top D(\overline{\mathbf{w}}-\mathbf{w})$ is negative, (18) is satisfied if and only if matrix $L(\mathbf{u},D,\overline{\gamma})$ is positive semi-definite, $L(\mathbf{u},D,\overline{\gamma})\succeq 0$.

Moreover, the linear inequality constraints (9c) are also stacked and processed by the SDPR method in a similar manner shown above. Let us define stacked vectors of upper and lower boundaries of (15) such that $\underline{\mathbf{f}}\le\mathbf{f}\le\overline{\mathbf{f}}$. Then, taking the upper boundary as an example:

$$\widetilde{C}_f x_0+\widetilde{D}_{fu}\mathbf{u}+\widetilde{D}_{fd}\mathbf{w}\le\overline{\mathbf{f}}. \tag{21}$$

The subtraction between the linear constraint (9c) and the upper bound (15) are described as follows:

$$e_i^\top\mathbf{f}-e_i^\top\overline{\mathbf{f}}=e_i^\top\widetilde{C}_f x_0+e_i^\top\widetilde{D}_{fu}\mathbf{u}+e_i^\top\widetilde{D}_{fd}\mathbf{w}-e_i^\top\overline{\mathbf{f}}\le 0, \tag{22}$$

where e_i is a vector whose ith element equals to 1 and the rest of the elements are assigned to zero, and $i\in\{1,2,\ldots,N+1\}$.

By applying the SDPR method on (22), the LMI of linear constraint (9c) with respect to the upper bound (15) can be found as $L_u(\mathbf{u},D_{u,i})$ based on the following equation:

$$\begin{aligned}&e_i^\top\mathbf{f}-e_i^\top\overline{\mathbf{f}}=-(\mathbf{w}-\underline{\mathbf{w}})^\top D_{u,i}(\overline{\mathbf{w}}-\mathbf{w})-\\&\begin{bmatrix}\mathbf{w}^\top & 1\end{bmatrix}\underbrace{\begin{bmatrix}D_{u,i} & -D_{u,i}\frac{\mathbf{w}+\overline{\mathbf{w}}}{2}-\frac{\widetilde{D}_{fd}^\top e_i}{2}\\ * & \underline{\mathbf{w}}^\top D_{u,i}\overline{\mathbf{w}}-e_i^\top\widetilde{C}_f x_0-e_i^\top\widetilde{D}_{fu}\mathbf{u}+e_i^\top\overline{\mathbf{f}}\end{bmatrix}}_{L_u(\mathbf{u},D_{u,i})}\begin{bmatrix}\mathbf{w}\\1\end{bmatrix},\end{aligned} \tag{23}$$

where $D_{u,i}$ is a positive semi-definite diagonal matrix ($0\preceq D_{u,i}\in\mathbb{R}^{N\times N}$). Since $-(\mathbf{w}-\underline{\mathbf{w}})^\top D_{u,i}(\overline{\mathbf{w}}-\mathbf{w})$ is negative, $e_i^\top\mathbf{f}-e_i^\top\overline{\mathbf{f}}\le 0$ is satisfied if and only if matrix $L_u(\mathbf{u},D_{u,i})$ is positive semi-definite, $L_u(\mathbf{u},D_{u,i})\succeq 0$.

Similarly to the deduction of $L_u(\mathbf{u},D_{u,i})$, the LMI of (9c) with respect to the lower bound can also be determined by:

$$\begin{aligned}&e_i^\top\mathbf{f}-e_i^\top\underline{\mathbf{f}}=-(\mathbf{w}-\underline{\mathbf{w}})^\top D_{l,i}(\overline{\mathbf{w}}-\mathbf{w})-\\&\begin{bmatrix}\mathbf{w}^\top & 1\end{bmatrix}\underbrace{\begin{bmatrix}D_{l,i} & -D_{l,i}\frac{\mathbf{w}+\overline{\mathbf{w}}}{2}-\frac{\widetilde{D}_{fd}^\top e_i}{2}\\ * & \underline{\mathbf{w}}^\top D_{u,i}\overline{\mathbf{w}}-e_i^\top\widetilde{C}_f x_0-e_i^\top\widetilde{D}_{fu}\mathbf{u}+e_i^\top\underline{\mathbf{f}}\end{bmatrix}}_{L_l(\mathbf{u},D_{l,i})}\begin{bmatrix}\mathbf{w}\\1\end{bmatrix},\end{aligned} \tag{24}$$

where $D_{l,i}$ is a negative semi-definite diagonal matrix ($0\succeq D_{l,i}\in\mathbb{R}^{N\times N}$). Since $-(\mathbf{w}-\underline{\mathbf{w}})^\top D_{l,i}(\overline{\mathbf{w}}-\mathbf{w})$ is positive, $e_i^\top\mathbf{f}-e_i^\top\underline{\mathbf{f}}\ge 0$ is satisfied if and only if matrix $L_l(\mathbf{u},D_{l,i})$ is negative semi-definite, $L_l(\mathbf{u},D_{l,i})\preceq 0$.

To summarise, the RMPC problem can be expressed as a convex optimisation, as follows:

$$\begin{aligned}\overline{\phi}=\min_{\mathbf{u}}\{&\overline{\gamma}\text{: the LMIs } L(\mathbf{u},D,\overline{\gamma})\succeq 0\ (20),\ L_u(\mathbf{u},D_{u,i})\succeq 0\ (23),\\&L_l(\mathbf{u},D_{l,i})\preceq 0\ (24),\ \text{and the convex constraint (9d) are}\\&\text{satisfied, for some variables: } 0\preceq D\in\mathbb{R}^{N\times N},\\&0\preceq D_{u,i}\in\mathbb{R}^{N\times N},\ 0\succeq D_{l,i}\in\mathbb{R}^{N\times N}\}.\end{aligned}$$

IV. Simulation Results

The performance of the proposed RMPC on the vehicle following scenario is evaluated in this section. The speed profile of the reference vehicle in the following adopts the extra high stage of the worldwide harmonised light vehicles test cycles (WLTP) to emulate high-way driving, with its average speed set as the cruise speed $\bar{v}$ (see Fig. 3).

To begin with, it is important to verify that the equality condition (6b) is held at all times. The representative case of $W_3 \ll W_1 + W_2$ shows this to be the case in Fig. 4. This example implies the validity of the formulation, which shows that the tightness is held across all horizons. Hence, the feasibility of the convexified solution in (6b) is verified.

The numerical evaluation of the proposed RMPC method is performed in two steps: 1) a comparison between the RMPC and a nominal MPC method with the same vehicle dynamics model and the cost function under the same initial conditions and disturbance; 2) an investigation on the impact of the horizon length and the amplitude of the disturbance. All the convex optimisation problems are solved by the CVX toolkit with MOSEK solver in the Matlab environment on a 1.6 GHz Dual-Core Intel Core i5 processor with 8 GB memory. The sampling interval of the solver is kept the same for all cases at $\Delta s = 40$ m, which strikes a balance between numerical accuracy and computation burden.

The first case considered is with a prediction horizon set to $N=5$. The optimal inter-vehicular time gap, Δt, solved by the RMPC method is compared in Fig. 5, with the solutions of the nominal MPC. As it can be seen, when there is a small disturbance ($\overline{v_w}=0.5\ m/s$), both nominal and robust controllers can maintain a safe Δt over the entire simulation. As the amplitude of the disturbance increases to $\overline{v_w}=2.0\ m/s$, the time gap of the nominal MPC is still within the desired safety gap due to some inherent robustness because of the feedback-loop in the MPC framework. However, further increase on the disturbance to $\overline{v_w}=2.6\ m/s$ eventually makes the nominal MPC infeasible while the RMPC framework is able to counter the impact of the external disturbance. Time gap plots of different disturbances managed by the RMPC are on top of each other, which is shown in the bottom of Fig 5. Further simulations (not shown here) demonstrate that the RMPC controller can tolerate disturbances at least as high as $\overline{v_w}=3.9\ m/s$, thus validating its additional robustness as compared to nominal MPC.

To further investigate the performance of the RMPC, the energy consumption is evaluated with different prediction horizon lengths ($N=3$ to $N=12$) and disturbance limits ($\overline{v_w}=0.5\ m/s$ to $\overline{v_w}=2.5\ m/s$). It can be seen in Fig. 6 that when

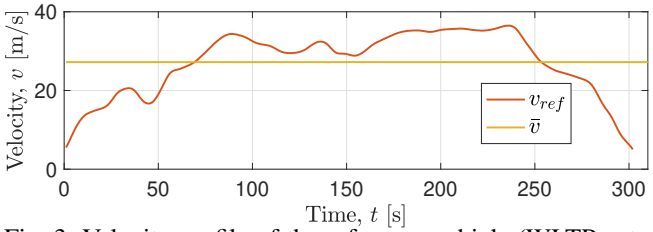

Fig. 3: Velocity profile of the reference vehicle (WLTP extra high), v_{ref}, and the constant cruise velocity, $\bar{v}$.

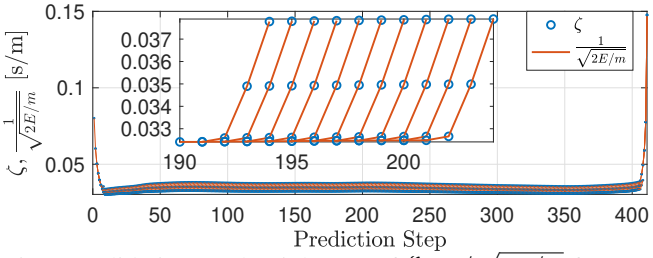

Fig. 4: Validation on the tightness of $\zeta \geq 1/\sqrt{2E/m}$ from an example solution of the convex RMPC with $W_3 \ll W_1 + W_2$.

$N=5$ there are significant energy savings for four disturbance limit cases at roughly 40%, as compared to the result with $N=3$. This can be understood that extending the prediction horizon initially enhances the ability to anticipate future behaviour of the reference vehicle, which leads to more optimal solutions. However, when N is further increased, the optimality of the RMPC with small disturbance limit $\overline{v_w}=0.5\ m/s$ has trivial improvement, while the rest of the disturbance cases have worse optimality in terms of energy cost or infeasible solutions (for example, the $\overline{v_w}=2.5\ m/s$ at $N=10$ is infeasible) due to the decreased accuracy of the reference vehicle velocity prediction and aggregated impact of the external disturbances. Although extending the prediction horizon length could improve the energy savings in some cases, as described just above, the computational burden is also increased, as shown in Table II. As we can see, as

TABLE II: Average computational time of various RMPC horizon length from $N=3$ to $N=12$, with the same disturbance limit $\overline{v_w}=0.5\,m/s$.

Prediction horizon length, N	3	5	8	10	12
Average computational time [s]	1.02	1.37	1.93	2.45	3.09

compared to the result with $N=3$, the computational time of the optimal solution with $N=5$ is increased by 34% but with a 40% reduction in energy cost (see Fig. 6). Further extension of the horizon length can barely improve the energy saving

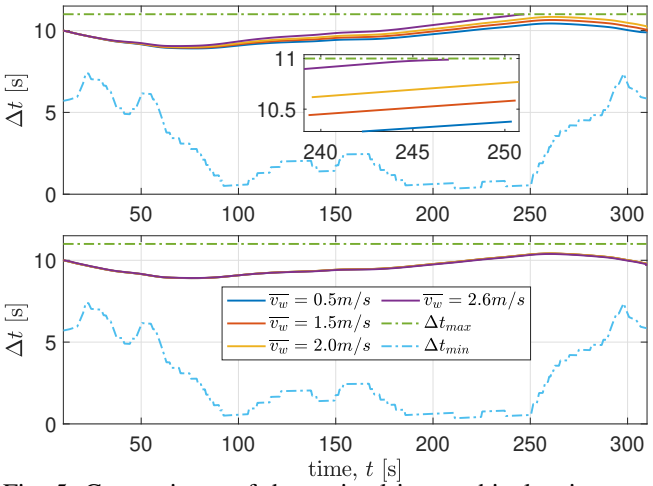

Fig. 5: Comparisons of the optimal inter-vehicular time gap Δt between the nominal MPC (top) and RMPC (bottom) with a prediction horizon $N=5$.

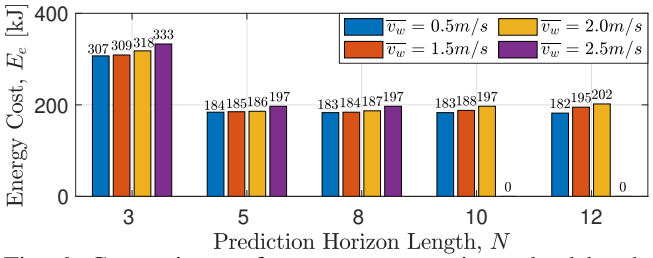

Fig. 6: Comparisons of energy consumption solved by the RMPC with different N and $\overline{v_w}$.

while instead the computational burden is increased up to 202% in the case of $N=12$. Thus, by carefully selecting the prediction horizon length N, the energy consumption can be significantly reduced and the computational burden can still be within an acceptable range for potential implementation.

V. Conclusion and Future Work

This paper proposes a convex robust model predictive control (RMPC) with semi-definite programming relaxation (SDPR) method to optimise energy efficiency in a vehicle following problem. Minimisation of controlled vehicle energy consumption as well as of the difference between the controlled vehicle speed and a constant cruise speed in traffic, subject to relevant constraints, are guaranteed under the influence of external disturbances. Moreover, a comparison between the proposed RMPC and a nominal MPC is conducted to demonstrate the robustness of the RMPC in dealing with the impact of external disturbances. A further investigation of different RMPC prediction horizon lengths reveals that the energy consumption can be improved by roughly 40% by carefully selecting the prediction horizon length. Finally, an analysis of the computational time suggests the implementation potential of the proposed RMPC. Future work will be devoted to including additional powertrain and battery characteristics and more realistic traffic scenarios.

References

[1] J. Sanguesa, J. Barrachina, M. Fogue, P. Garrido, F. Martinez, J. Cano, C. Calafate, and P. Manzoni, "Sensing traffic density combining V2V and V2I wireless communications," *Sensors (Basel)*, vol. 15, no. 12, p. 31794–31810, 2015.

[2] J. Barrachina, J. A. Sanguesa, M. Fogue, P. Garrido, F. J. Martinez, J. Cano, C. T. Calafate, and P. Manzoni, "V2X-d: A vehicular density estimation system that combines V2V and V2I communications," in *2013 IFIP Wireless Days (WD)*, 2013, pp. 1–6.

[3] G. Marsden, M. McDonald, and M. Brackstone, "Towards an understanding of adaptive cruise control," *Transportation Research Part C: Emerging Technologies*, vol. 9, no. 1, pp. 33–51, 2001.

[4] L. Luo, H. Liu, P. Li, and H. Wang, "Model predictive control for adaptive cruise control with multi-objectives: Comfort, fuel-economy, safety and car-following," *Journal of Zhejiang University SCIENCE A*, vol. 11, p. 191–201, 2010.

[5] C. C. Chien and P. Ioannou, "Automatic vehicle-following," in *1992 American Control Conference*, 1992, pp. 1748–1752.

[6] D. Moser, R. Schmied, H. Waschl, and L. del Re, "Flexible spacing adaptive cruise control using stochastic model predictive control," *IEEE Transactions on Control Systems Technology*, vol. 26, no. 1, pp. 114–127, 2018.

[7] H. Chen, L. Guo, H. Ding, Y. Li, and B. Gao, "Real-time predictive cruise control for eco-driving taking into account traffic constraints," *IEEE Transactions on Intelligent Transportation Systems*, vol. 20, no. 8, pp. 2858–2868, 2019.

[8] H. Chu, L. Guo, B. Gao, H. Chen, N. Bian, and J. Zhou, "Predictive cruise control using high-definition map and real vehicle implementation," *IEEE Transactions on Vehicular Technology*, vol. 67, no. 12, pp. 11 377–11 389, 2018.

[9] S. Li, K. Li, J. Wang, L. Zhang, X. Lian, H. Ukawa, and D. Bai, "MPC based vehicular following control considering both fuel economy and tracking capability," in *2008 IEEE Vehicle Power and Propulsion Conference*, 2008, pp. 1–6.

[10] A. Khodayari, A. Ghaffari, M. Nouri, S. Salehinia, and F. Alimardani, "Model predictive control system design for car-following behavior in real traffic flow," in *2012 IEEE International Conference on Vehicular Electronics and Safety (ICVES 2012)*, 2012, pp. 87–92.

[11] B. Sakhdari and N. L. Azad, "Adaptive tube-based nonlinear mpc for economic autonomous cruise control of plug-in hybrid electric vehicles," *IEEE Transactions on Vehicular Technology*, vol. 67, no. 12, pp. 11 390–11 401, 2018.

[12] G. Gunter, C. Janssen, W. Barbour, R. E. Stern, and D. B. Work, "Model-based string stability of adaptive cruise control systems using field data," *IEEE Transactions on Intelligent Vehicles*, vol. 5, no. 1, pp. 90–99, 2020.

[13] B. Sakhdari, E. M. Shahrivar, and N. L. Azad, "Robust tube-based mpc for automotive adaptive cruise control design," in *2017 IEEE 20th International Conference on Intelligent Transportation Systems (ITSC)*, 2017, pp. 1–6.

[14] S. Feng, H. Sun, Y. Zhang, J. Zheng, H. X. Liu, and L. Li, "Tube-based discrete controller design for vehicle platoons subject to disturbances and saturation constraints," *IEEE Transactions on Control Systems Technology*, vol. 28, no. 3, pp. 1066–1073, 2020.

[15] X. Lin and D. Görges, "Robust model predictive control of linear systems with predictable disturbance with application to multiobjective adaptive cruise control," *IEEE Transactions on Control Systems Technology*, vol. 28, no. 4, pp. 1460–1475, 2020.

[16] S. Zhang, Y. Luo, J. Wang, X. Wang, and K. Li, "Predictive energy management strategy for fully electric vehicles based on preceding vehicle movement," *IEEE Transactions on Intelligent Transportation Systems*, vol. 18, no. 11, pp. 3049–3060, 2017.

[17] M. Vajedi and N. L. Azad, "Ecological adaptive cruise controller for plug-in hybrid electric vehicles using nonlinear model predictive control," *IEEE Transactions on Intelligent Transportation Systems*, vol. 17, no. 1, pp. 113–122, 2016.

[18] Y. Kaijiang and J. Yang, "Performance of a nonlinear real-time optimal control system for hevs/phevs during car following," *Journal of applied mathematics*, vol. 2014, p. 1–14, 2014.

[19] B. Chen, X. Pan, S. A. Evangelou, and S. Timotheou, "Optimal control for connected and autonomous vehicles at signal-free intersections," *IFAC-PapersOnLine*, vol. 53, no. 2, pp. 15 306–15 311, 2020.

[20] A. Loulizi, Y. Bichiou, and H. Rakha, "Steady-state car-following time gaps: An empirical study using naturalistic driving data," *Journal of Advanced Transportation*, vol. 2019, pp. 1–9, 2019.

[21] M. Wang, W. Daamen, S. P. Hoogendoorn, and B. van Arem, "Rolling horizon control framework for driver assistance systems. part i: Mathematical formulation and non-cooperative systems," *Transportation Research Part C: Emerging Technologies*, vol. 40, pp. 271–289, 2014.

[22] C. B. Math, A. Ozgur, S. H. de Groot, and H. Li, "Data rate based congestion control in v2v communication for traffic safety applications," in *2015 IEEE Symposium on Communications and Vehicular Technology in the Benelux (SCVT)*, 2015, pp. 1–6.

[23] X. Pan, B. Chen, and S. A. Evangelou, "Optimal vehicle following strategy for joint velocity and energy management control of series hybrid electric vehicles," *IFAC-PapersOnLine*, vol. 53, no. 2, pp. 14 161–14 166, 2020.

[24] B. Chen, S. A. Evangelou, and R. Lot, "Series hybrid electric vehicle simultaneous energy management and driving speed optimization," *IEEE/ASME Transactions on Mechatronics*, vol. 24, no. 6, pp. 2756–2767, 2019.

[25] S. Uebel, N. Murgovski, B. Bäker, and J. Sjöberg, "A two-level mpc for energy management including velocity control of hybrid electric vehicles," *IEEE Transactions on Vehicular Technology*, vol. 68, no. 6, pp. 5494–5505, 2019.

[26] F. Tahir and I. M. Jaimoukha, "Causal state-feedback parameterizations in robust model predictive control," *Automatica*, vol. 49, pp. 2675–2682, 2013.

[27] A. Georgiou, F. Tahir, S. A. Evangelou, and I. M. Jaimoukha, "Robust moving horizon state estimation for uncertain linear systems using linear matrix inequalities," in *2020 59th IEEE Conference on Decision and Control (CDC)*, 2020, pp. 2900–2905.

[28] A. Georgiou, S. A. Evangelou, I. M. Jaimoukha, and G. Downton, "Tracking control for directional drilling systems using robust feedback model predictive control," *IFAC-PapersOnLine*, vol. 53, no. 2, pp. 11 974–11 981, 2020.